

Large Eddy Simulation of a complete Harrier aircraft in ground effect

G. J. Page

J. J. McGuirk

g.j.page@lboro.ac.uk

j.j.mcguirk@lboro.ac.uk

Department of Aeronautical Engineering

Loughborough University

Loughborough, UK

ABSTRACT

This paper aims to demonstrate the viability of using the large eddy simulation (LES) CFD methodology to model a representative, complete STOVL aircraft geometry at touch down. The flowfield beneath such a jet-borne vertical landing aircraft is inherently unsteady. Hence, it is argued in the present work that the LES technique is the most suitable tool to predict both the mean flow and unsteady fluctuations, and, with further development and validation testing, this approach could be a replacement, and certainly a complementary aid, to expensive rig programmes. The numerical method uses a compressible solver on a mixed element unstructured mesh. Examination of instantaneous flowfield predictions from these LES calculations indicate close similarity with many flow features identified from ground effect flow visualisations, which are well known to be difficult to model using RANS-based CFD. Whilst significant further work needs to be carried out, these calculations show that LES could be a practical tool to model, for example, Hot Gas Ingestion for the Joint Strike Fighter aircraft.

1.0 INTRODUCTION

The flowfield surrounding a vertical landing aircraft is a complex interaction of headwind-driven onset flow, multiple lift jet ground impingement, ground sheet 3D wall jets, upwash fountain flow, and ground vortex flow, see Fig. 1. Although some attempts have been made to predict vertical landing aircraft aerodynamics using Reynolds Averaged Navier Stokes (RANS) CFD methods, success

has been limited due to the inability of RANS-based statistical turbulence models to capture the complex flow physics sufficiently accurately. A recent review of jet induced effects for STOVL aircraft in hover and transition⁽¹⁾ has summarised the history of attempts to apply CFD techniques in this type of application. It is clear that, although since the 1980s there has been much research into applying CFD methods to component flows relevant to STOVL aircraft, e.g. jets in crossflow, jets in ground effect, etc., much less work has been reported for complete aircraft simulations. Partly this is due to the extreme complexity (and fundamentally 3D unsteady nature) of the flow phenomena of interest (particularly hot gas ingestion, HGI), and partly to the challenge of generating large grids for the complex geometry of a whole aircraft, and the associated high computational storage and run-time costs. Early attempts used simplified models⁽²⁾, and the most ambitious attempts so far were published in 2002⁽³⁻⁵⁾. This work focussed heavily on the need for shorter solution time and automation of the grid generation, flow solution and post-processing steps. Little attention was paid to the physical accuracy of the solutions. Whilst unsteady computations were reported, there must be serious doubts about the ability of Unsteady RANS (URANS) methods to cope with the extreme unsteadiness of ground effect and HGI flowfields. This was recognised in Ref. 1., which pointed out that, for massively separated flows, the relatively immature CFD technique of Large Eddy Simulation (LES) (or related techniques such as Detached Eddy Simulation (DES)) offers much greater potential for representing the flow physics to higher fidelity than URANS. Indeed, promising results applying LES to component

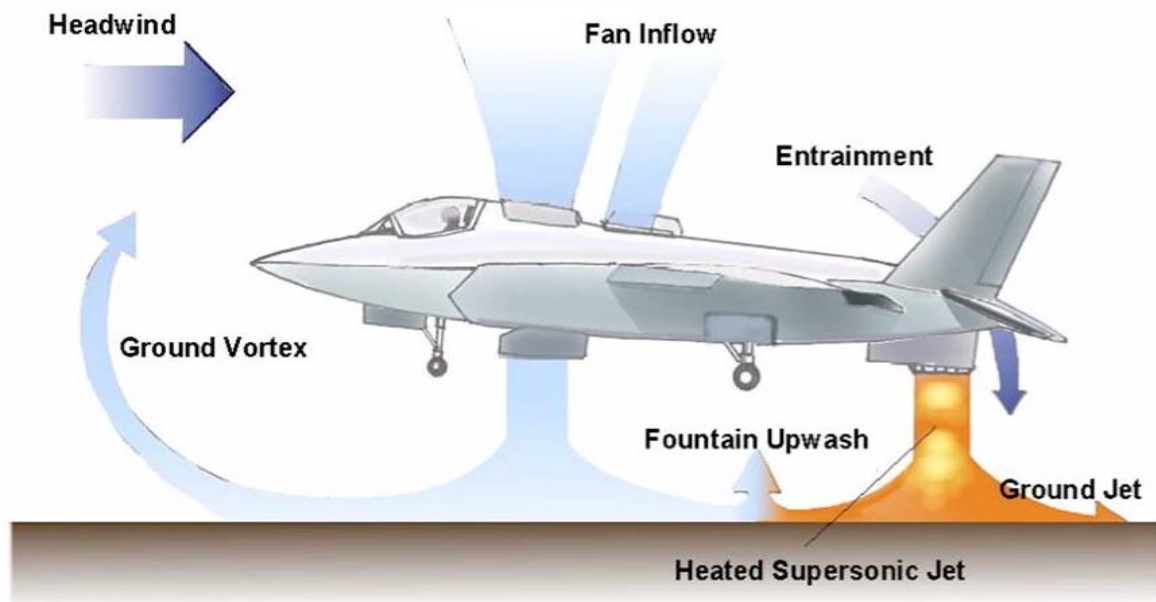


Figure 1. STOVL aircraft ground effect aerodynamics.

flowfields such as multiple impinging jets^(6,7) have already appeared. The Large Eddy Simulation CFD methodology is much more likely to be able to predict accurately both the mean and unsteady components of the flow that are so important in determining ground effect flow characteristics such as hot gas ingestion.

Traditionally, model scale rig tests have been used to develop STOVL aircraft, for example configurations which are less susceptible to HGI. However, experimental testing is expensive and provides only limited information on the flowfield (such as ground plane flow visualisation and intake temperature histories). This testing has led to the Harrier aircraft using 'strakes' and 'dams' under the fuselage to control the upwash fountain flow. CFD methods have the potential to complement or replace rig testing if they can be shown to model accurately ground effect aerodynamics such as the HGI problem. In particular, with aircraft such as the STOVL variant of the Joint Strike Fighter, it is possible that issues will occur in service that will need to be rapidly studied and circumvented using a validated CFD methodology. RANS CFD is unable to provide information on important phenomena such as the unsteady fountain and instantaneous flow distortion and swirl in the intake. The ability to predict both the mean flow and unsteady excursions is important for the design and development of future aircraft. LES resolves all of the large scale structures greater than the grid scale, and predicts temporal variation of the flow. The potential usefulness of LES for the prediction of the upwash fountain was shown in the 1980s with pioneering work by Childs and Nixon⁽⁸⁾ and Rizk and Menon⁽⁹⁾ which, although limited by available computing power, was extremely promising. Previous work by the current authors has used LES for simplified impinging jet flow problems that contained the important fountain and ground vortex flow features⁽¹⁰⁾. Comparison with experiment showed improved accuracy over RANS predictions as well as unsteady ingestion for a case with an intake.

Because of complex aircraft geometry, grid generation is always a challenge, and the current work uses a mixed element, unstructured solver to reduce the magnitude of this task. The unstructured grid approach is particularly useful in this type of problem where high resolution is required underneath the aircraft, whilst also handling features such as auxiliary intakes. Similarly, the combination of complex geometry and LES results in an extremely large

computational problem and it is imperative that calculations are carried out on large scale parallel computation facilities. The aim of this study is therefore to demonstrate the capability of LES when applied to a geometrically detailed Harrier aircraft near touch down. The work reported here complements the study of Richardson *et al*⁽¹¹⁾, which has demonstrated moving mesh unstructured URANS solutions for a descending aircraft using the same basic CFD code.

2.0 METHODOLOGY

2.1 Solution algorithm

The starting point for this work was the Rolls-Royce CFD code Hydra⁽¹²⁾. This is an unstructured, mixed element, compressible, density-based Reynolds Averaged Navier-Stokes solver. To convert this code to solve in an LES format, the temporal and spatial discretisation were improved so as to avoid excessive dissipation of resolved eddies. In particular the added 2nd and 4th order smoothing terms were modified to include a monitor based on both local vorticity and divergence; this keeps the basic scheme as close as possible to central differencing, but still allows some upwind terms near shock waves. Sub-grid-scale models were also incorporated. The important features are summarised below; further details of the discretisation and testing on simpler LES flow problems can be found in Tristante *et al*⁽¹³⁾.

2.2 Governing equations

Employing Cartesian vector decomposition and using conservative variables (ρ , ρu , ρv , ρw , E), the governing time dependent equations in terms of the spatially filtered compressible Navier-Stokes equations can be expressed in volume integral form as:

$$\frac{\partial}{\partial t} \iiint_V Q dV + \iint_{\partial V} F(Q) \cdot n dS + \iint_{\partial V} G(Q) \cdot n dS = 0 \quad \dots (1)$$

where the dependent variable vector \mathbf{Q} and the inviscid flux vector $\mathbf{F}(\mathbf{Q})$ are defined as:

$$\mathbf{Q} = \begin{bmatrix} \bar{\rho} \\ \bar{\rho}\tilde{\mathbf{u}} \\ \bar{\rho}\tilde{\mathbf{v}} \\ \bar{\rho}\tilde{\mathbf{w}} \\ \tilde{\mathbf{E}} \end{bmatrix}, \quad \mathbf{F}(\mathbf{Q}) \cdot \mathbf{n} = \begin{bmatrix} \bar{\rho}\tilde{U}_n \\ \bar{\rho}\tilde{U}_n\tilde{\mathbf{u}} + n_x\bar{p} \\ \bar{\rho}\tilde{U}_n\tilde{\mathbf{v}} + n_y\bar{p} \\ \bar{\rho}\tilde{U}_n\tilde{\mathbf{w}} + n_z\bar{p} \\ \tilde{U}_n(\tilde{\mathbf{E}} + \bar{p}) \end{bmatrix}, \quad \dots (2)$$

where \tilde{U}_n is the mass carrying velocity and $\mathbf{G}(\mathbf{Q})$ contains viscous and conduction flux (i.e. SGS model) terms. An overbar denotes unweighted filtered variables and a tilde denotes density-weighted filtered variables. The spatial filter corresponds to the control volume surrounding the node. The finite volumes are created from the median-dual of an original body-fitted unstructured mesh, which may contain tetrahedra, hexahedra, pyramids and prisms.

2.3 Discretisation

For an edge ij that connects nodes i and j in the grid, the flux is computed using the second-order accurate scheme of Moinier⁽¹⁴⁾:

$$F_{ij} = \frac{1}{2} [F(\mathbf{Q}_i) + F(\mathbf{Q}_j) - \text{smoothing}], \quad \dots (3)$$

The smoothing term is defined as⁽¹²⁾:

$$\text{Smoothing} = |A_{ij}| \varepsilon_1 (L_j^p(\mathbf{Q}) - L_i^p(\mathbf{Q})), |A_{ij}| = \partial F / \partial \mathbf{Q} \quad \dots (4)$$

where L is the pseudo-Laplacian. For LES it is essential that the smoothing term should be kept as small as possible so as to avoid unphysical dissipation of the resolved eddies. This is achieved by the use of the sensor function of Ducros *et al.*⁽¹⁵⁾ to control ε_1 , based upon the vorticity Ω and divergence $(\nabla \cdot \mathbf{u})$:

$$\varepsilon_1 = \max \left(\varepsilon_2, \varepsilon_3 \frac{(\nabla \cdot \mathbf{u})^2}{(\nabla \cdot \mathbf{u})^2 + \Omega^2} \right) \quad \dots (5)$$

where ε_2 and ε_3 are user defined parameters. The sensor increases the level of smoothing for regions of high divergence and reduces it to a base level of ε_2 for regions of high vorticity. In some cases, particularly at jet impingement, unphysical oscillations were observed in the near wall region and the smoothing was locally increased in the cells closest to the wall to damp the oscillations. Temporal discretisation used a third order accurate, three-stage Runge-Kutta algorithm.

2.4 Sub-grid scale (SGS) model

The standard Smagorinsky SGS model defines the subgrid scale viscosity μ , appearing in the non-resolved sub-grid-scale stresses in the $\mathbf{G}(\mathbf{Q})$ term as:

$$\mu_1 = C_s^2 \rho \Delta^2 \sqrt{2S_{ij}S_{ij}}, S_{ij} = \frac{1}{2} \left(\frac{\partial \tilde{u}_i}{\partial x_j} + \frac{\partial \tilde{u}_j}{\partial x_i} \right). \quad \dots (6)$$

where (using Cartesian tensor notation) S_{ij} is the resolved scale strain rate and Δ is the filter width (cube root of the local cell volume). For the correct prediction of the low Reynolds number viscous sublayer of a turbulent flow, the SGS model viscosity should tend to zero in such regions. This is not true for a fixed-coefficient Smagorinsky model, in particular in the near wall region where the term becomes large. An improvement on the basic Smagorinsky model is the wall-adapting local eddy-viscosity

(WALE) SGS model proposed by Nicoud and Ducros⁽¹⁶⁾ for LES in complex geometries. This model behaves correctly in low turbulence regions, where it has been shown to be independent of near-wall distance, with a natural recovery of sublayer flow conditions without an explicit damping function. This is therefore the SGS model adopted here; for further details see Nicoud & Ducros⁽¹⁶⁾.

2.5 Parallel implementation

The complex aircraft geometry and the fine mesh required to resolve as much of the dynamically important turbulent eddy length scales as possible at the high Reynolds numbers found in practice necessarily leads to a large number of grid points. Coupled with the need to run for a large number of time steps to obtain statistically stationary flow, and also because of the disparity in time scales between the smallest and largest eddies, it follows that LES calculations for high Reynolds number complex aerodynamic flows are not feasible on single processor machines and must be run on large scale parallel facilities to achieve a reasonable turnaround time. Whilst structured multiblock CFD codes are relatively straightforward to implement in parallel, making use of the block structure to achieve domain decomposition, an unstructured solver requires an efficient partitioning strategy and careful handling of the message passing to achieve good efficiency on large numbers of processors. The present unstructured solver uses the OPLUS library⁽¹⁷⁾, with message passing implemented in MPI. The partitioning is carried out in parallel using the ParMetis library. More information is provided by Hills⁽¹⁸⁾, who describes how the parallel implementation has been tuned for large scale problems; near linear speed-up has been demonstrated by Hills⁽¹⁸⁾ for up to 1024 processors on an IBM Power⁽⁵⁾ system.

3.0 SIMPLE TEST CASE

3.1 Twin impinging jet with intake in cross-flow

Detailed flowfield experimental data for VSTOL aircraft in ground effect are scarce. Hence, the measurements of Behrouzi and McGuirk⁽¹⁹⁾ were used as a first test case. The geometry is much simpler than a complete aircraft, but a combination of twin impinging jets, a crossflow and an intake system make the flow problem fluid mechanically representative of the major components of a STOVL aircraft ground effect flowfield. The geometry is shown in Fig. 2 via a dimensioned sketch of the experimental set up (using the jet nozzle exit diameter D_j as a reference length scale), and a close-up view of a solid model of the twin vertical jet pipes with the intake located in between. The relative location of ground plane, jet height and spacing, and intake position is similar to a Harrier aircraft at the wheels-on condition. The experiment was carried out in a horizontal water tunnel to facilitate non-intrusive LDA measurements of the mean and turbulent flow fields. There are clearly therefore no compressibility effects, but the high Reynolds number turbulence conditions ensure similarity in terms of highly unsteady features such as a fountain and a ground vortex. The flow condition corresponding to a velocity ratio $R = V_j/U_c$ (impinging jet vertical velocity divided by crossflow axial velocity) of 24 and an impingement height of $7 D_j$ gave intermittent ingestion of the jet fluid into the intake and was chosen for simulation. The jet Reynolds number based on exit velocity and nozzle diameter was 40,000; only a brief description of the results is provided here, more details may be found in Li *et al.*⁽⁷⁾.

An unstructured mesh of ~1.8 million cells was generated, as shown in Fig. 3. The mesh contains a region of hexahedral cells with high density in the region between the jet exits and the ground

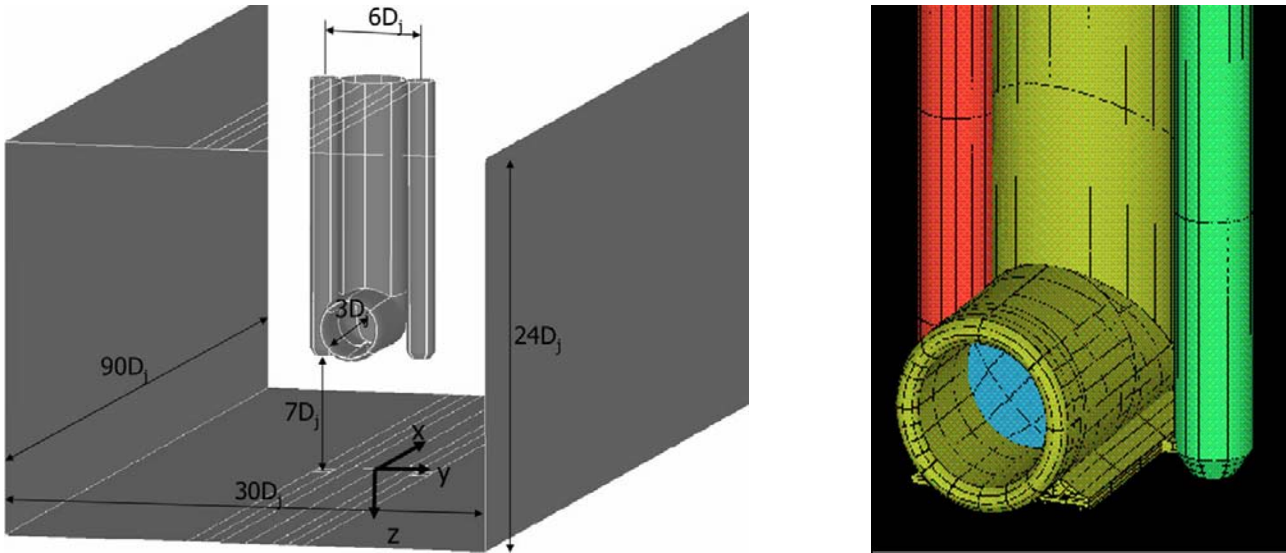


Figure 2. Geometry of twin impinging jet in crossflow with intake test case.

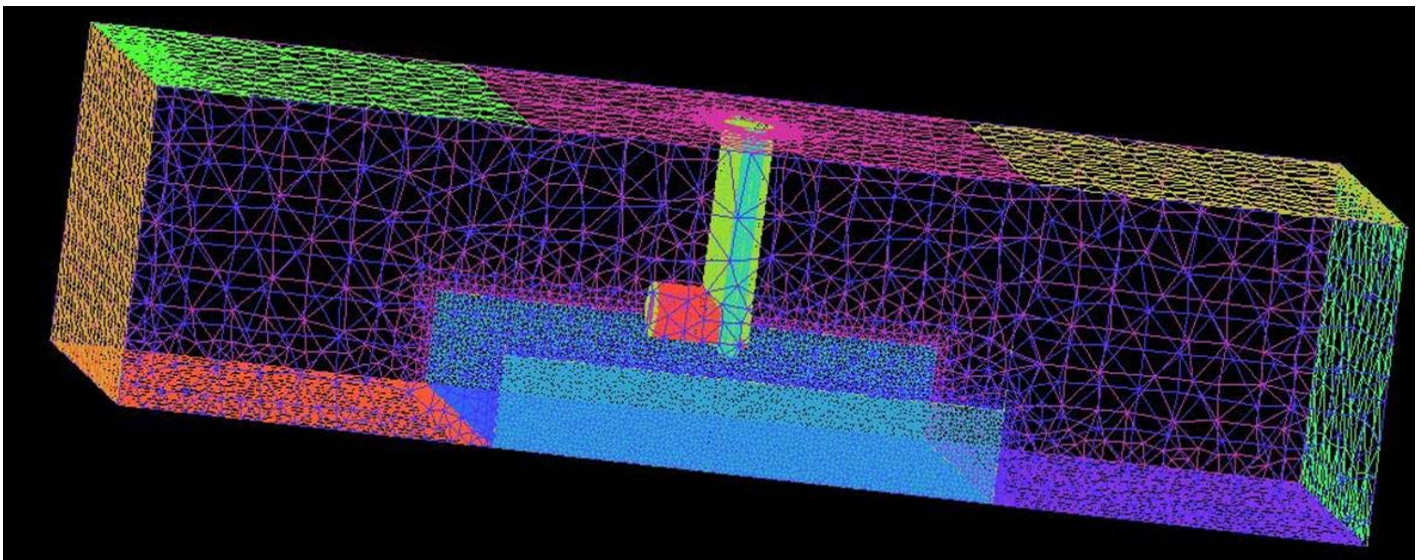


Figure 3. Mesh for twin impinging jet in crossflow with intake test case.

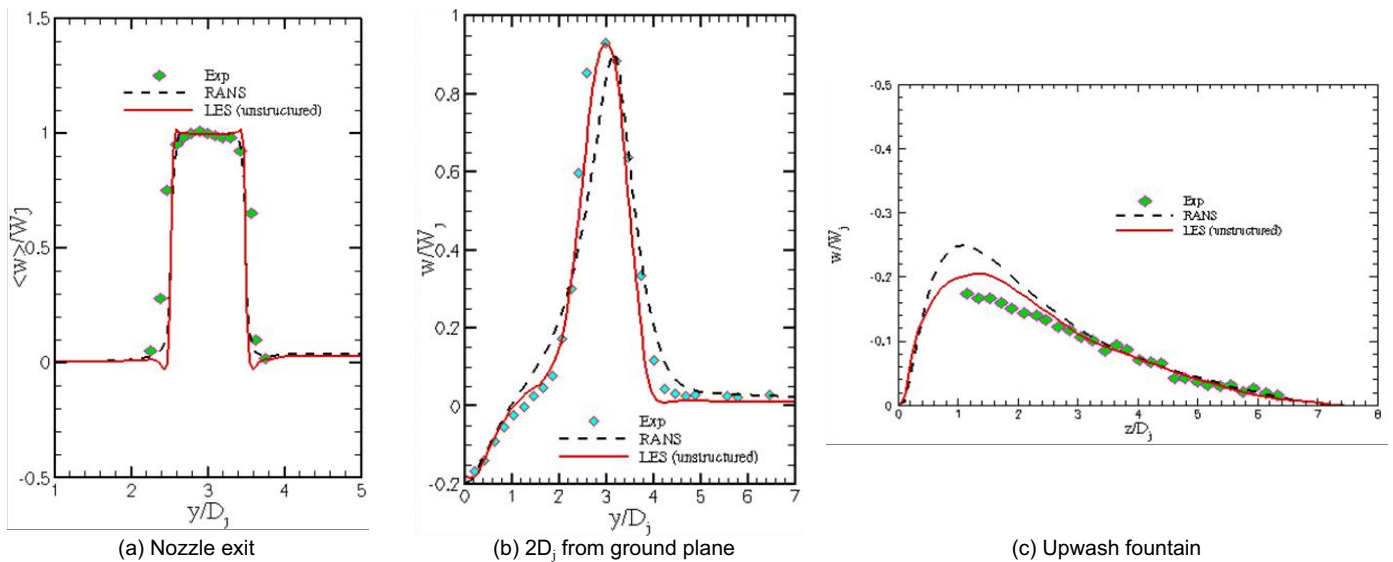


Figure 4. Comparison between LES and RANS predicted and measured vertical velocity profiles.

plane and where the ground vortex region is expected. Away from this zone, tetrahedral elements are used to ease grid generation near the intake and jet pipe structures, and allow expansion towards the water tunnel side and upper walls.

3.2 Results

Figure 4 provides typical comparisons between mean velocities evaluated by time-averaging the LES predictions after reaching a statistically stationary state and the experimental data. The agreement is very good, particularly for the profile in the upwash fountain, which is known to be difficult for RANS models to predict because of its unsteady behaviour. The LES simulation predicts the correct jet spread and the correct fountain strength and width. In general there is an improvement when changing to LES from RANS CFD. A better impression of the highly fluctuating flow is given via instantaneous snapshots of the flow. Figures 5 and 6 show two views of instantaneous contours of a conserved scalar quantity discharged from the jet nozzles.

The scalar is set to a value of unity in the jets and a zero value in the crossflow. Intermediate values therefore indicate the level of mixing between jet and crossflow fluid. Figure 5 illustrates the leading edge of the ground vortex and the ingestion of jet fluid into the intake after impingement of the fountain flow on the intake undersurface, whilst Fig. 6 clearly shows the impinging jets and the upwash fountain. A video of this simulation shows the intermittent nature of the ingestion process.

4.0 COMPLETE HARRIER AIRCRAFT IN GROUND EFFECT TEST CASE

4.1 Geometry, flow conditions and mesh

Unlike the previous test case, which was effectively incompressible and with unheated jets, the complete Harrier aircraft test case has four high Mach number compressible hot jets and a low speed ambient temperature crossflow. In addition the geometry is substantially more complicated, including strakes and dams to control the upwash fountain, auxiliary doors, and deflected flaps. Figure 7 shows a 1/15 scale model Harrier, based on the mould lines of the AV-8B/GR-7, located in a test cell at Rolls-Royce (Bristol). The lower half of the model is fully detailed, but above the plane of the nozzles, simplifications have been made in order to allow the correct feed of air to the nozzles and extraction of air from the intake. The model includes

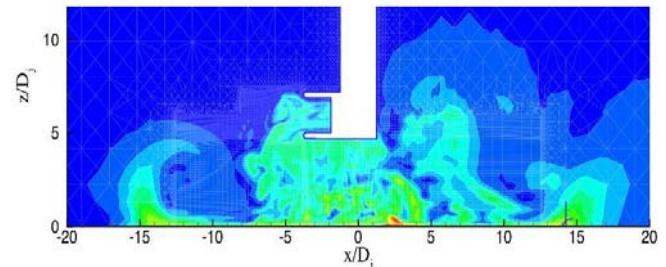


Figure 5. Instantaneous scalar contours in intake symmetry plane.

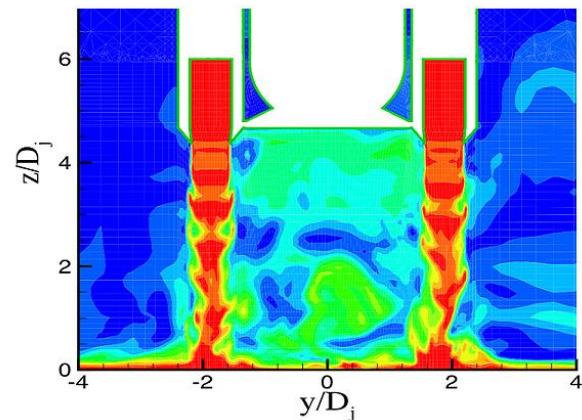


Figure 6. Instantaneous scalar contours in jet impingement plane.

auxiliary intake blow-in doors, longitudinal strakes and transverse dams. Whilst the model shown in the figure includes undercarriage and gun-pods, these were not included in the CFD geometry. The aircraft fuselage datum is at a 7.50 nose up angle to the ground plane. The centre of the intake is 0.59m from the ground plane and is representative of an aircraft whose wheels are about to touch the ground.

Model testing uses scaling laws and the flow conditions tested and used to provide boundary conditions for the LES calculation are not necessarily representative of the full scale aircraft. The rear jets were specified with a total temperature of 700K and a Nozzle Pressure Ratio of 2.0. The temperature of the front jets is 350K and a Nozzle Pressure Ratio of 2.5. These NPR values are sufficiently high that the convergent nozzles are choked and the jets are therefore mildly under-expanded. The approximate dimensions of the non-circular nozzles are 21 × 28mm (front) and 38 × 42mm (rear). The jet Reynolds numbers



Figure 7. Two views of 1/15th scale model Harrier.

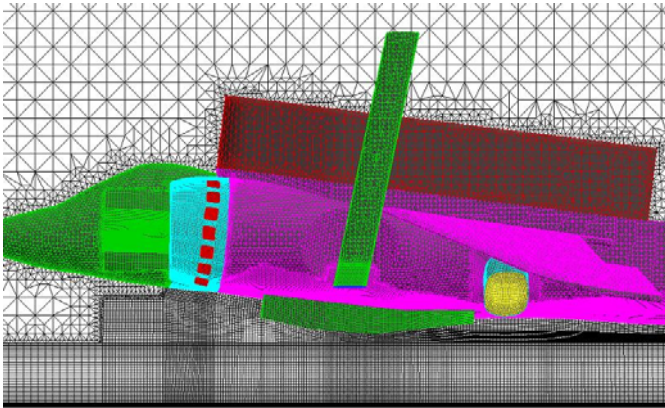


Figure 8. Mesh for scale model Harrier – side view.

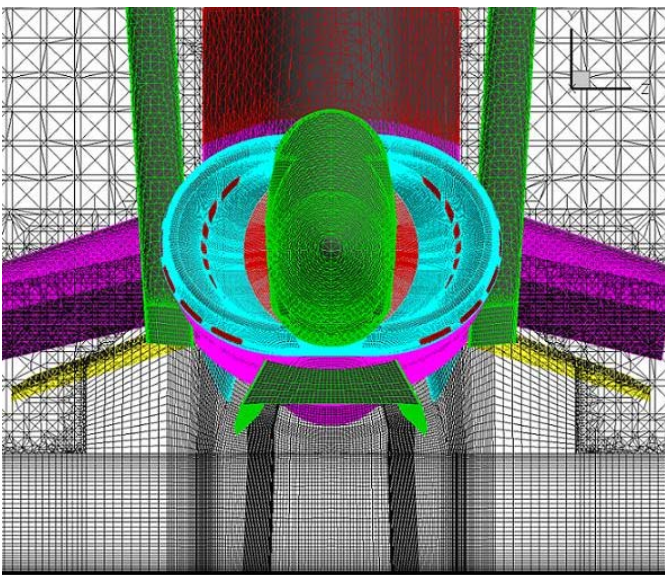


Figure 9. Mesh for scale model Harrier – front view.

are 8 million (front) and 7 million (rear). In both cases the Reynolds number is based on jet exit conditions and the largest dimension of the non-circular nozzles. The crossflow is set at 6m/s and the intake static pressure is set to 3kPa below ambient.

The mesh is of a mixed element type and is generated using the ICM Hexa package. The majority of the elements underneath the aircraft are hexahedral, with tetrahedral elements used to handle the complex rig geometry at the top of the aircraft. Hexahedral elements were also used in the main and auxiliary intakes. O-mesh features were used to capture the jet nozzles. The nozzle internal flow was not meshed – only flow downstream of the nozzle exit planes was predicted. Whilst RANS predictions for an un-yawed aircraft can exploit symmetry and only model half the aircraft, LES must always allow for fully 3D flow, which is instantaneously asymmetric and the complete aircraft must be modelled. Consequently, the mesh contains 17.3 million nodes with 22.6 million elements, of which 15.7 million are hexahedral. The mesh spacing in the near wall region and jet shear layers was set to be similar to that found to be acceptable in earlier simulations of simplified impinging jet problems⁽¹⁰⁾. The coordinate system is set such that the nose of the aircraft is at $x = 0$ with the domain extending forward by 3m and aft by 3m. The spanwise (z) extent is set to 1.956m each side of the aircraft centreline and the height (y) of the solution domain is 2.184m. The mesh is illustrated in Figs 8 and 9 and more details of similar meshes used for URANS predictions may be found in Richardson *et al.*⁽¹¹⁾. Preliminary calculations of this Harrier configuration using the

same mesh and an earlier version of the LES code contain more details of the computational set-up, see Page *et al.*⁽²⁰⁾.

4.2 Computational demand

The LES solutions presented below have run for approximately 130,000 time steps at a time step of 7×10^{-8} s (after some start-up running to allow initial conditions to be 'forgotten'). The small time step is due to the high speed (supersonic) jets and the fine mesh resolution. The present calculations were run on the UK National HECToR Cray XT-3 system on just 64 processors. With this level of compute resource, throughput was 1,200 time steps per hour of wallclock time, and the calculations presented here were completed in an elapsed time of two weeks. Although this corresponds to only ~10ms of real time at model scale (around 0.15s at full scale), this is roughly the same as the residence time for a fluid particle which leaves the jets to enter the intake. Whilst this is long enough to provide good capture of the unsteady flow physics underneath the aircraft, around ten times longer running would be needed if statistically converged time-averaged data were required. However, if 4 times the number of processors were used, since the CFD methodology used here will scale roughly linearly for these processor numbers, then even an LES calculation to obtain time-averaged information would take only around five weeks. These numbers are significant, since 256 processors are fairly commonly available in medium size PC clusters in today's computing environments, and, given the quantity and quality of insight into the unsteady aerodynamics obtained, the elapsed time is considered acceptable, even in an industrial context. Clearly LES is not the right methodology for regular design calculations, but for selected problems, where fidelity at the unsteady aerodynamic level is essential (such as the HGI problem), it is argued here that it is the best CFD methodology to adopt, and, although expensive, its use is justified.

4.3 Predicted flowfield

Once again, a video is the best way to appreciate the full power of the time-domain information provided by the LES prediction. However, instantaneous snapshots in selected planes do communicate some of the unsteady features of the simulation reasonably well. Figures 10 and 11 present instantaneous snapshots of Mach contours at four selected planes: the diametral plane through the rear jets and a plane midway between front/rear jets (Figs 10(a) and 10(b)), and the front jets plane and a plane near the front of the dam (Figs 11(a) and 11(b)).

Features which are clearly visible in these pictures are: the expected highly unsteady nature of the fountain flow, being angled sometimes to the right (Figs 10(a), 11(a)), sometimes vertically up (Fig. 11(b)) and sometimes to the left (Fig. 10(b)); the higher Mach numbers in the front compared to the rear jets; the thin and highly convoluted ground sheet layer; and finally the way the upwash fountain is captured and channelled back downwards by the strakes/dam (Fig. 11(b)). For the front jets the strakes shield the inner jet shear layers from the fountain for about half their trajectory towards the ground plane, but the high turbulence in the fountain then causes the inner jet shear layer to spread much more rapidly than the outer (Fig. 11(a)).

Similarly, the instantaneous contours of stagnation temperature shown in Figs 12 and 13 help to visualise the hot gas ingestion process. The hot (700K) rear jets are clearly visible in Fig. 12(a); mixing reduces the gas temperature, but the upwards moving fountain flow is still around 600K at this plane. Most of this hot gas is of course prevented from approaching the intake after impingement on the aircraft undersurface by the strakes and dam. At the front jet plane (Fig. 12(b)) the gas temperature is around 400K, and the capture/shielding effect of the strakes and dam is still visible.

Moving forward to a plane on the edge of the dam, although the temperature has now dropped even further, the first evidence of gas evading capture by the strakes/dam is seen (Fig. 13(a)). Finally, at the

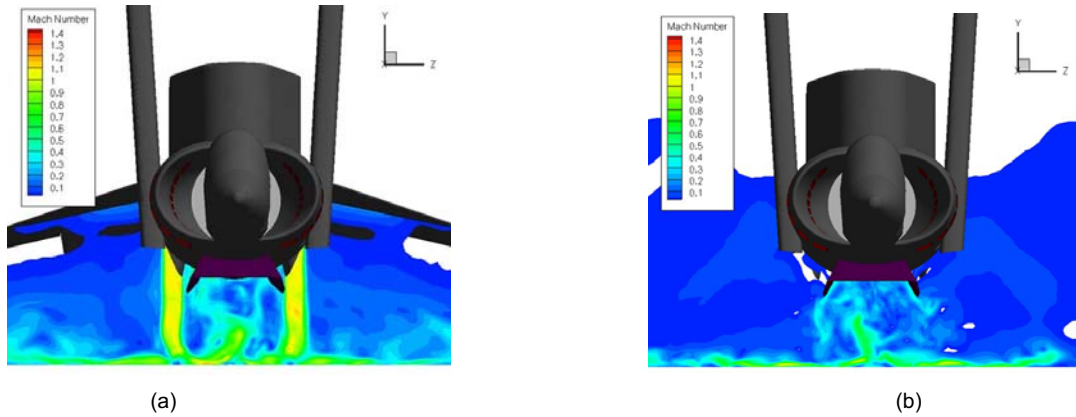


Figure 10. Instantaneous Mach contours: rear jets plane (left) between front/rear jets (right).

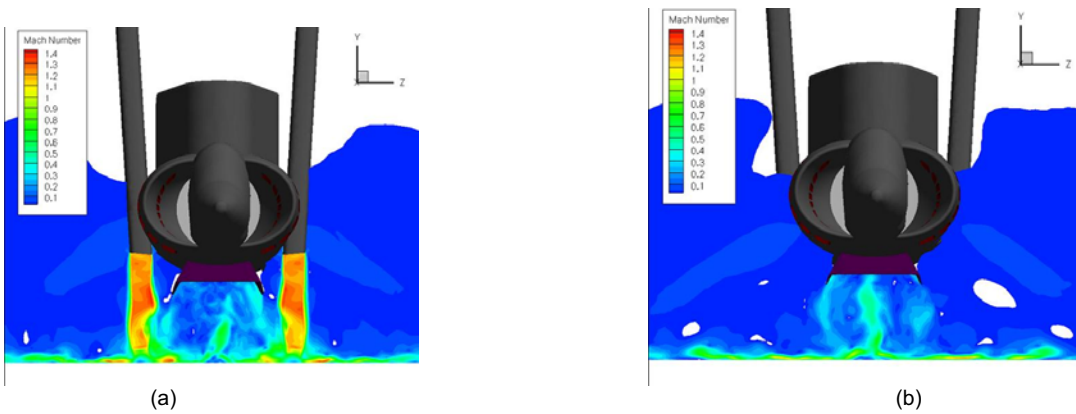


Figure 11. Instantaneous Mach contours: front jets plane (left), near front of dam plane (right).

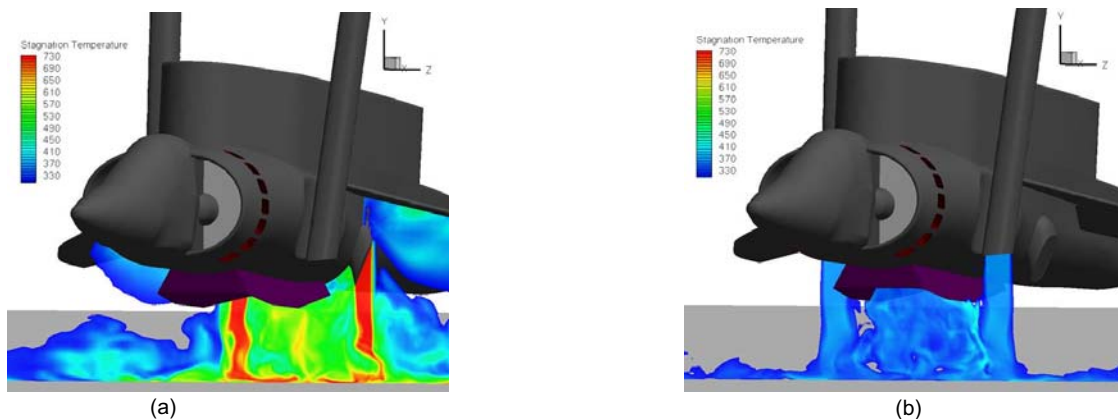


Figure 12. Instantaneous stagnation temperature contours: rear jets plane (left), front jets plane (right).

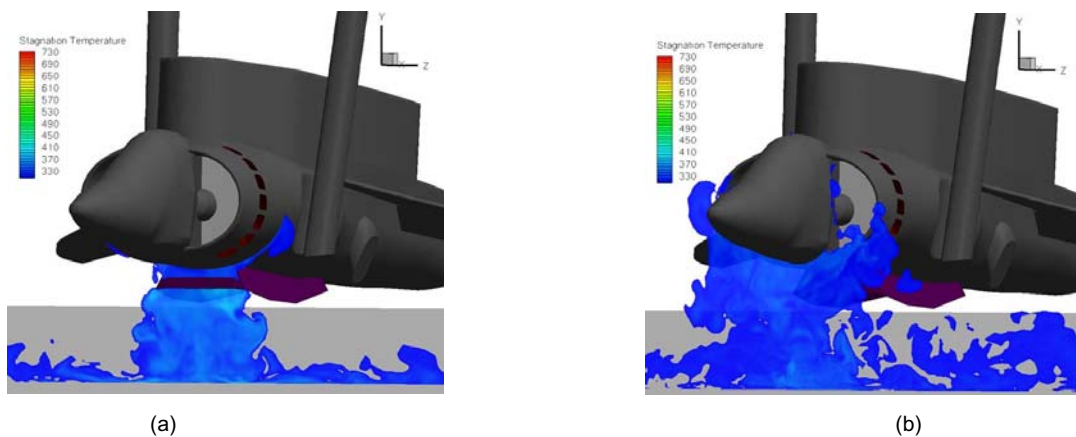


Figure 13. Instantaneous stagnation temperature contours: edge of dam plane (left), intake face plane (right).

intake plane, the large turbulent eddy structures created near the top edge of the ground vortex flow are seen to be responsible for ingestion (Fig.13(b)).

Finally, since the LES method produces a fundamentally unsteady solution, and compressible flow equations have been solved, then acoustic waves excited by the jets and their impingement on the ground plane are also an inherent part of the simulation. Although with the grid used at present these waves will be damped by the rather coarse mesh as they propagate away from the primary noise source region in the vicinity of the jets, the unsteady pressure field predicted in the simulation still gives a clear picture of the creation and radiation way from the aircraft near-field of these waves, as shown in Fig. 14. Such information is potentially of great value in estimating near-field aircraft component fatigue problems, or the in-ground-effect noise environment to which personnel may be exposed with high pressure impinging jet operation.

8.0 CONCLUSIONS

A successful Large Eddy Simulation of a model representing a full Harrier aircraft geometry at touch down has been carried out using a parallel unstructured CFD algorithm. Important phenomena have been observed in the instantaneous flow, in particular the highly energetic and hence highly unsteady turbulent structures which affect fountain flow behaviour. The influence of the strakes and dam on controlling the upwash fountain was clearly visible, as was the origin of the hot gas which eventually enters the intake. Whilst there is still much work to be done to confirm the quantitative accuracy of the time-dependent features revealed in the LES predictions, the results show that LES of complete aircraft configurations is possible. Although such simulations are computationally expensive, the cost is decreasing with time, and it is argued here that this approach can become a practical tool to model HGI for STOVL aircraft. There is currently no other CFD technique which offers the possibility of sufficient fidelity of simulation of the complex turbulent flow physics in ground effect flows to serve as a complementary tool to support rig test programmes.

ACKNOWLEDGMENTS

Funding for this project was provided by the UK Engineering and Physical Sciences Research Council (EPSRC) via Grant GR/S21021/01. The computer time was provided through the UK Applied Aerodynamics Consortium (UKAAC) under EPSRC grant

GR/S91130/01. The authors would like to thank Dr. Nick Hills at the University of Surrey for guidance on setting up the parallel simulations, and Dr Qinling Li for her contribution to the impinging jet problem and to preliminary calculations of the Harrier problem. The authors thank BAE Systems (Warton) and Rolls Royce(Bristol) for providing constructive comments at all stages of the work.

REFERENCES

1. KUHN, R.E., MARGASON, R.J. and CURTIS, P. Jet Induced Effects: the Aerodynamics of Jet and Fan Powered V/STOL Aircraft in Hover and Transition, *Progress in Astronautics and Aeronautics*, **217**, Lu, F.K., (Ed), AIAA Publication, 2006.
2. ROTH, K.R., Comparison of CFD with experiment for a geometrically simplified STOVL model, AIAA-96-2431, 1996.
3. CHADERJIAN, N.M., PANDYA, S.A., AHMAD, J.U. and MURMAN, S.C. Parametric time-dependent Navier Stokes computations for a YAV-8B Harrier in Ground Effect, AIAA-2002-0950, 40th AIAA Aerospace Sciences Meeting, Reno, Nevada, USA, January 2002.
4. PANDYA, S.A., CHADERJIAN, N.M. and AHMAD, J. Parametric study of a YAV-8B Harrier in ground effect using time-dependent Navier Stokes computations, AIAA-2002-3056, 20th AIAA Applied Aerodynamics Conference, St Paul, Miss, USA, June 2002.
5. CHADERJIAN, N.M., PANDYA, S.A., AHMAD, J. AND MURMAN, S.C. Progress towards generation of a Navier-Stokes database for a Harrier in ground effect, AIAA-2002-5966, International Powered Lift Conference, Williamsburg, Virginia, USA, November 2002.
6. TANG, G., YANG, Z., PAGE, G.J. and MCGUIRK, J.J. Simulation of an Impinging Jet in Crossflow Using an LES Method, AIAA-2002-5939, Int. Powered Lift Conf, Williamsburg, Virginia, USA, 2002.
7. LI, Q., PAGE, G.J. and MCGUIRK, J.J. Large eddy simulation of twin impinging jets in cross-flow, *Aeronaut J*, March 2007, **111**, pp 195–206.
8. CHILDS, R. and NIXON, D. Unsteady three-dimensional simulations of a VTOL upwash fountain, AIAA-86-0202, 24th AIAA Aerospace Sciences Meeting, Reno, Nevada, USA, January 1986.
9. RIZK, M. and MENON, S. An investigation of excitation effects on a row of impinging jets using large-eddy simulations, AIAA-88-0043, 26th AIAA Aerospace Sciences Meeting, Reno, Nevada, USA, January 1988.
10. PAGE, G.J., LI, Q. and MCGUIRK, J.J. LES of impinging jet flows relevant to vertical landing aircraft, AIAA-2005-5226, 23rd AIAA Computational Flow Dynamics Conference, Toronto, Ontario, Canada, June 2005.
11. RICHARDSON, G., DAWES, W. AND SAVILL, M. Unsteady, moving mesh CFD simulation applied to Harrier VSTOL aircraft for hot-gas ingestion control analysis, *Aeronaut J*, March 2007, **111**, pp 133–144.
12. CRUMPTON, P.I., MOINIER, P. and GILES, M.G. An unstructured algorithm for high Reynolds number flows on highly stretched grids, Tenth International Conference on Numerical Methods for Laminar and Turbulent Flow, 1997.
13. TRISTANTO, I. H., LI, Q., PAGE, G.J. and MCGUIRK, J.J. On the Effect of Convective Flux Formation for LES of Compressible Flows using Hybrid Unstructured Meshes, AIAA-2006-54940, 36th AIAA Fluid Dynamics Conference, San Francisco, California, USA, June 2006.
14. MOINIER, P. Algorithm Developments for an Unstructured Viscous Flow Solver, Ph.D. thesis, University of Oxford, Oxford, UK, 1998.
15. DUCROS, F., FERRAND, V., NICOU, F., WEBER, C., DARRACQ, D., GACHERIU, C. and POINSOT, T. Large-eddy simulation of the shock/turbulence interaction, *J Computational Physics*, 1999, **152**, pp 517–549.
16. NICOU, F. and DUCROS, F. Sub grid-scale stress modelling based on the square of the velocity gradient tensor, *Flow, Turbulence and Combustion*, 1999, **62**, pp 183–200.
17. BURGESS, D., CRUMPTON, P. and GILES, M. A parallel framework for unstructured grid solvers, in: *Programming Environments for Massively Parallel Distributed Systems*, DECKER K.M. and REHMANN R.M., (Eds) Birkhauser, 1994.
18. HILLS, N. Achieving high parallel performance for an unstructured unsteady turbomachinery code, *Aeronaut J*, March 2007, **111**, pp 185–193.
19. BEHROUZI, P. and MCGUIRK, J.J. Experimental data for CFD validation of the intake ingestion process in STOVL aircraft, *Flow Turbulence and Combustion*, 2000, **64**, pp 233–251.
20. PAGE, G.J., LI, Q. and MCGUIRK, J.J. Large eddy simulation of a Harrier aircraft at touch down, AIAA 2007-4294, 25th AIAA Applied Aerodynamics Conference, Miami, Florida, USA, June 2007.

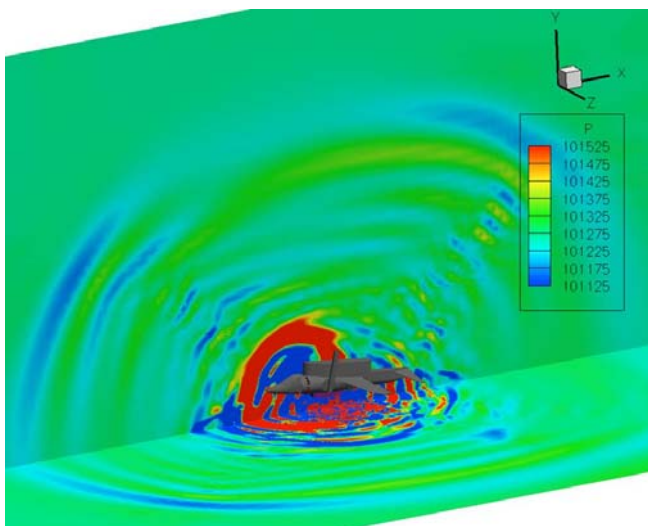


Figure 14. Instantaneous pressure field, showing acoustic waves radiating to far-field.